Biosensors and Bioelectronics 26 (2010) 1353–1358

Contents lists available at ScienceDirect

Biosensors and Bioelectronics

journal homepage: www.elsevier.com/locate/bios

Nonenzymatic free-cholesterol detection via a modified highly sensitive macroporous gold electrode with platinum nanoparticles

Yi-Jae Lee, Jae-Yeong Park*

Department of Electronic Engineering, Kwangwoon University, 447-1 Wolgye-Dong, Nowon Gu, Seoul 139-701, Republic of Korea

ARTICLE INFO

Article history:
Received 14 April 2010
Received in revised form 12 July 2010
Accepted 13 July 2010
Available online 21 July 2010

Keywords:
Macroporous Au
Pt nanoparticles
Macroporous Au-/nPts
Electroplating
Nonenzymatic
Free-cholesterol

ABSTRACT

A sensitive macroporous Au electrode with a highly rough surface obtained through the use of with Pt nanoparticles (macroporous Au-/nPts) is reported. It has been designed for nonenzymatic free-cholesterol biosensor applications. A macroporous Au-/nPts electrode was fabricated by electroplating Pt nanoparticles onto a coral-like shaped macroporous Au electrode structure. The macroporous Au-/nPts electrode was physically characterized by field emission scanning electron microscopy (FESEM). It was confirmed that the Pt nanoparticles were well deposited on the surface of the macroporous Au electrode. The porosity and window pore size of the macroporous Au electrode were 50% and 100–300 nm, respectively. The electroplated Pt nanoparticle size was approximately 10–20 nm. Electrochemical experiments showed that the macroporous Au-/nPts exhibited a much larger surface activation area (roughness factor (RF) = 2024.7) than the macroporous Au electrode (RF = 46.07). The macroporous Au-/nPts also presented a much stronger electrocatalytic activity towards cholesterol oxidation than does the macroporous Au electrode. At 0.2 V, the electrode responded linearly up to a 5 mM cholesterol concentration in a neutral media, with a detection limit of 0.015 mM and detection sensitivity of 226.2 $\mu A\,mM^{-1}\,cm^{-2}$. Meanwhile, interfering species such as ascorbic acid (AA), acetaminophen (AP), and uric acid (UA), were effectively avoided. This novel nonenzymatic detection electrode has strong applications as an electrochemically based cholesterol biosensor.

1. Introduction

Cholesterol and its fatty acid esters are one of the main constituents of mammalian cell membranes and precursors of other biological materials, such as bile acid and steroid hormones. Estimation of cholesterol in blood is considered as a very important parameter for the diagnosis and prevention of several kinds of heart disease, hypertension, arteriosclerosis, cerebral thrombosis and other disorders that require continuous monitoring of blood cholesterol (Solanki et al., 2009; Malhotra and Chaubey, 2003; Shumyantseva et al., 2004). The normal concentration of cholesterol in human serum is in the range of −5.17 mM, of which 30% is present as sterol and 70% is esterified with fatty acids (MacLachlan et al., 2000), along with various interfering species, such as uric acid and ascorbic acid. Cholesterol level is commonly determined by employing nonenzymatic spectrophotometric techniques, using colored substances. This method, however, involves complex procedures for the precipitation of lipoproteins fractions and suffers from various drawbacks, such as low specificity, instability of reagents and high cost. It is thus desirable and crucial to develop techniques for cost-effective, convenient, rapid, sensitive and selective estimation of cholesterol levels in blood. Therefore, various electrochemical methods have been used for cholesterol assays (Khan et al., 2009).

Several electrochemical cholesterol detection electrodes including enzymatic and nonenzymatic methods have been reported (Solanki et al., 2009; Brahim et al., 2001; Srivastava et al., 2000). However, these often have certain difficulties like lack of specificity and selectivity due to the presence of various interfering reactions and the use of unstable and corrosive reagents. Recent efforts have been focused on using enzymes immobilized on electrodes for electrochemical detection (Martin et al., 2003). Immobilization of enzymes is generally carried out either by direct physical adsorption or through mediators or entrapment in polymers (Brahim et al., 2001). There is no doubt that the use of enzymes in the fabrication of sensor electrodes has obvious advantages, but the stability of the sensor electrode is mainly affected by the stability of the enzymes, which are easily affected by temperature, humidity, pH, etc. Unlike the enzyme-based electrode, a nonenzymatic detection electrode has several attractive advantages, such as stability, simple fabrication, reproducibility, low cost, and freedom from oxygen limitation (Park et al., 2006).

* Corresponding author. Tel.: +82 2 940 5113; fax: +82 2 942 1502.
E-mail address: jaepark@kw.ac.kr (J.-Y. Park).

0956-5663/$ – see front matter © 2010 Elsevier B.V. All rights reserved.
doi:10.1016/j.bios.2010.07.048

Especially, in order to achieve a truly nonenzymatic electrode, the fabrication of porous structured electrodes is very promising in electrochemical sensing applications. The main characteristics of such porous electrodes in the electro-analytical domains are their high surface/volume ratio, thereby being favourable for the interaction with external reagents, excellent conductivity, and the interconnectivity between the pores, which makes them very attractive for the miniaturization of electrochemical devices (Szamocki et al., 2007). If they are electrically conducting, such materials deposited as thin films on other electrode surfaces can contribute to an increase in the electro-active surface area by several orders of magnitude, with a commensurate enhancement in the sensitivity of the resulting device.

Meanwhile, nano-sized metal particles have been used for several impressive applications such as catalysis, sensors (Bonnemann and Waldofner, 2002). However, these nanoparticles need the supporting material which enables them to be highly dispersed and stable. Pt nanoparticles supported on carbon nanotubes, TiO_2, and carbon were also employed as high-efficiency electrocatalysts (Cao et al., 2007). The Pt or Pt-based nanoparticles are still indispensable and are shown to be the most effective option for the enhancement of electrocatalytic activity at present. The electrocatalytic activity of the Pt particles is dependent on many factors, such as particle size and dispersion (Katsuaki et al., 1990), preparation methods (Loffler et al., 2001), and the supporting materials (Gloaguen et al., 1997). Furthermore, the activity of the catalyst is strongly dependent on the structure of the supporting materials (Yu et al., 2002). Supporting materials with large surface area are essential in order to reduce the Pt loading under the condition of maintaining the high catalytic activity. The supporting materials also promote electron transfer and demonstrate catalytic activity for many electrochemical reactions. Additionally, the macroporous electrode and nanoparticles can be used effectively for developing a highly sensitive biosensor.

In this paper, we first present a macroporous Au electrode with a coral-like shape and a highly rough surface achieved through the use of Pt nanoparticles (macroporous Au-/nPts). This electrode is intended for extremely high sensitive and selective nonenzymatic free-cholesterol detection. The open interconnected macroporous structures of the three-dimensional Au electrode provides an efficient means of enlarging the surface area and ensuring accessibility of the reactants to the surface active sites in the electrodes. The Pt nanoparticles are also promising for the enhancement of the surface roughness and electrochemical catalytic activity. The macroporous Au electrode is fabricated by the use of a templating method. The Pt nanoparticles are then formed on the surface of the macroporous Au electrode by the use of a nonionic surfactant and electroplating technique. The surface morphology of the fabricated macroporous Au-/nPts was checked by the use of a field emission scanning electron microscope (FESEM). Also, the macroporous Au-/nPts electrode was characterized in a sulfuric acid solution for the purposes of monitoring its surface roughness by cyclic voltammetry. In order to evaluate its electrochemical catalytic characteristic and applicability, the macroporous Au-/nPts electrode was characterized in various cholesterol concentrations with interfering species, respectively.

2. Experimental

2.1. Reagents

All the chemicals used were analytical reagent grade. All solutions were prepared with deionized water (resistivity ≥18 MΩ-cm). The aluminum precursor (aluminum sec-butoxide), surfactants (stearic acid and magnesium stearate), gold precursor ($HAuCl_4$), acid etchant (mixture of 11.8 M H_3PO_4 and 0.6 M HNO_3), and sodium tetrahydridoborate ($NaBH_4$) were prepared for the coral-like macroporous Au electrode (Kim et al., 2009). The electroplating mixture for the Pt nanoparticles was comprised of 42% (w/w) $C_{16}EO_8$ (octaethylene glycol monohexadecyl ether, 98% purity, Fluka), 29% (w/w) deionized water (18 MΩ-cm) and 29% (w/w) HCPA (hexachloroplatinic acid hydrate, 99.9% purity, Aldrich) (Attard et al., 1997).

The surface roughness of the fabricated electrode was measured in a 1 M sulfuric acid (H_2SO_4, 95–98%, ACS, Sigma–Aldrich) solution by the use of cyclic voltammograms. A 1 M H_2SO_4 solution was prepared by dilution in deionized water. The cholesterol, Triton X-100, and 2-propanol were purchased from Sigma–Aldrich. The cholesterol did not dissolve well in a standard buffer solution. So, surfactant Triton X-100 and 2-propanol were used to enhance the solubility of the cholesterol in the preparation of a cholesterol containing solution. After homogenization, the volume was made up to 100 ml with a 0.1 M phosphate buffered saline (PBS, pH 7.0) and thermostated at 35 °C (Kumar et al., 2001). The 0.1 M ascorbic acid (AA, 98%, Sigma), acetaminophen (AP, 99%, Sigma), and uric acid (UA, 99%, Sigma) were prepared by diluting them in a phosphate buffered saline (PBS, 0.1 M, pH 7.4) solution, respectively.

2.2. Apparatus

Electrochemical experiments were performed on the fabricated electrode at room temperature with the use of an electrochemical analyzer (Model 600B series, CH Instruments Inc., USA) at room temperature. A three-electrode system was used, including a fabricated electrode functioning as a working electrode, a flat Pt bar as a counter electrode, and an Ag/AgCl reference electrode with a 3 M NaCl solution, respectively. The surface morphology of the fabricated electrodes was characterized with a Hitachi S-4300 field emission scanning electron microscope (FESEM). Amperometric measurements were carried out in a 0.1 M PBS (pH 7.0, 20 ml volume) solution under continuous stirring by diluting the cholesterol (0.1 M) with a uniform concentration. The 0.1 M cholesterol was diluted in a 0.1 M PBS by controlling its injection volume, such as 0.015 mM (3 μl) and 0.5 mM (100.5 μl). The response current was recorded after stabilizing the background current at a nearly constant value and the prepared cholesterol was periodically injected at 50 s intervals.

2.3. Preparation of coral-like macroporous Au-/nPts

Fig. 1 represents a simplified fabrication sequence for the coral-like macroporous Au and Au-/nPts electrodes. As shown in Fig. 1(A), the coral-like macroporous Au was formed through the use of aggregated Au nanoparticles. A similar phase separation was found in the preparation of the monolithic TiO_2 via a template-free sol–gel process (Konishi et al., 2006). The aluminum precursor (Al sec-butoxide) and surfactants (stearic acid and magnesium stearate) were separately dissolved in sec-butyl alcohol. Au precursor ($HAuCl_4$) was added to a solution of the dissolving surfactant. These two solutions were mixed and followed by slow addition of water at the rate of 1 ml/min. $NaBH_4$ was used as a reducing agent for the Au precursor. Also the mixture was stirred continuously for 24 h. Subsequently the mixture was dried at 80 °C and calcined at 550 °C in air. At this calcination step, the surfactant was easily removed, and the resulting material had a nanoporous alumina structure with a sintered Au network. The alumina network with nanopores was etched selectively by etching with acid etchants (11.8 M H_3PO_4 and 0.6 M HNO_3). After etching, an additional heating process was conducted at 150 °C for 20 min in order to remove defects from the Au nanoparticles. Then the macroporous Au was obtained, namely, the reverse phase of the alumina network. The fabricated macroporous Au was pressed at room temperature into a

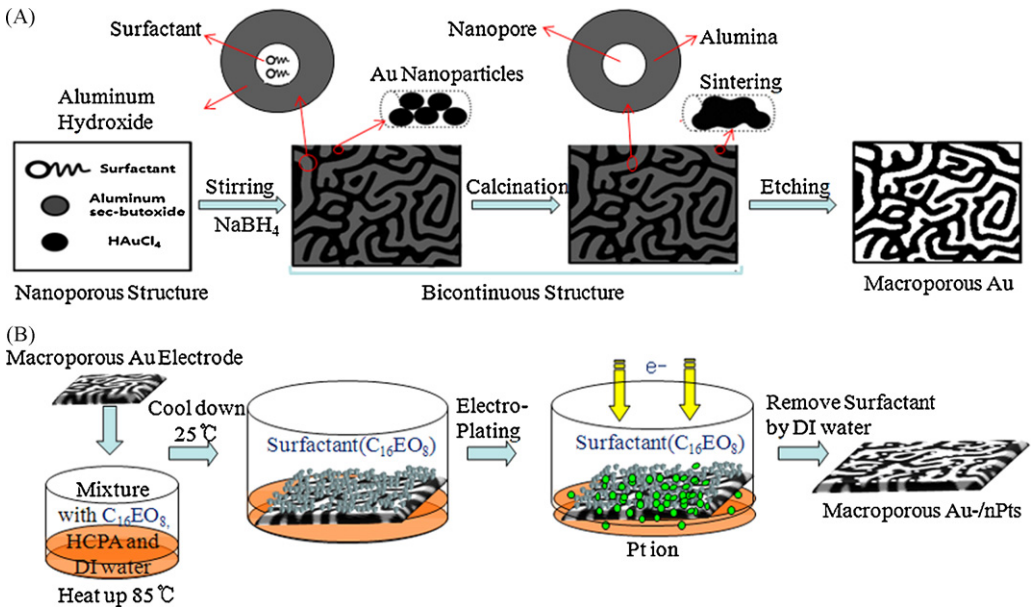

Fig. 1. Fabrication processes of macroporous Au (Kim et al., 2009) (A) and macroporous Au-/nPts (B) electrodes by templating method and electroplating technique.

circular mold for the purposes of making a sensor working electrode (applied pressure; 10 kgf cm^{-3}, mold radius; 3.5 mm).

Fig. 1(B) shows the fabrication sequences of the macroporous Au electrode with Pt nanoparticles. An electroplating mixture for forming the Pt nanoparticles was well mixed and heated up to 85 °C, after which the mixture became transparent and homogeneous. The macroporous Au electrode was dipped into the mixture and the temperature was lowered to 25 °C. At this stage, the liquid crystalline structure of the nonionic surfactant $C_{16}EO_8$ was formed on the surface of the macroporous Au electrode. Next, the Pt nanoparticles were electroplated on the macroporous Au electrode by means of a constant potential (−0.12 V *vs.* Ag/AgCl) and charge condition of 70 mC. The electrode was then soaked in distilled water for several hours to remove the $C_{16}EO_8$ (Lee et al., 2008). Finally, the macroporous Au electrode with Pt nanoparticles was formed.

3. Results and discussions

3.1. Surface morphology

The surface morphology of the fabricated coral-like macroporous Au electrode, after it had been electroplated with Pt nanoparticles, was examined by the use of FESEM. As shown in Fig. 2(A), the fabricated macroporous Au-/nPts had a coral-like structure. The primary branch with a ca. 2–3 μm size has the shape of a bumpy branch that resembles a one-directional link of spherical particles (ca. 200–400 nm), which are made up of aggregated Au nanoparticles (ca. 10–30 nm). The porosity and window pore size of the fabricated macroporous Au-/nPts were approximately 50% and 100–300 nm, respectively. Fig. 2(B) shows apparently formed Pt nanoparticles on the surface of the macroporous Au electrode. The Pt nanoparticles (white dots in Fig. 2B) were uniformly well electroplated on the macroporous Au electrode and exhibited sizes ranging from 10 to 20 nm. (The measured atomic ratios of Au and Pt by dispersive X-ray spectroscopy (JSM-6700F (Jeol)) were 91.88% and 8.12%, respectively.) The density and size of the Pt nanoparticles could be controlled by varying the charge condition of the electroplating process, since the electroplating current is the dominant influence in the formation of metal particles (Lee et al., 2008; Boonyongmaneerat et al., 2009). The FESEM images demonstrated that the macroporous Au-/nPts structure possesses a greatly enhanced surface roughness.

3.2. Roughness factor of the macroporous Au and Au-/nPts electrodes

In order to electrochemically characterize the real surface of the fabricated electrode, cyclic voltammogram measurements were performed in a 1 M H_2SO_4 solution. The cyclic voltammogram was obtained at a scan rate of 20 mV/s and the potential ranged from

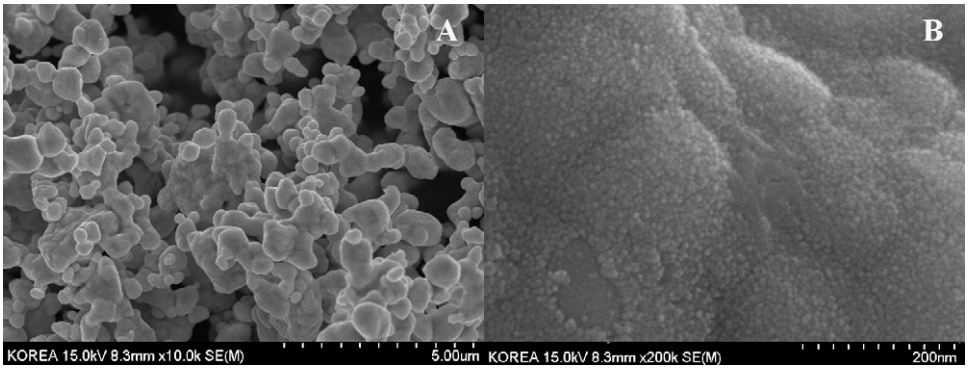

Fig. 2. FESEM images of macroporous Au-/nPts (A) and its close-up view (B).

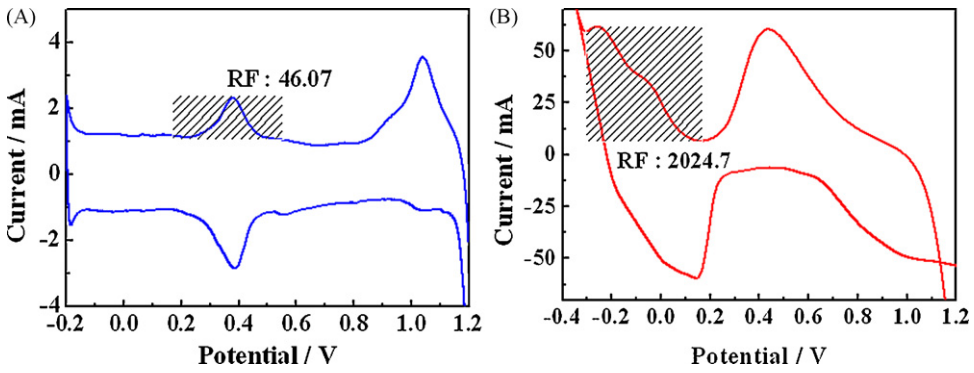

Fig. 3. Cyclic voltammograms of macroporous Au (A) and macroporous Au-/nPts (B) electrodes in 1 M sulfuric acid solution. Scan rate: 20 mV/s.

−0.4 V to 1.2 V *vs.* Ag/AgCl. The roughness factors (RFs) of these electrodes were calculated as follows (McNaught and Wilkinson, 1997):

$$\text{Roughness factor (RF)} : f_r = \frac{A_r}{A_g}$$

where A_r is the real (true, actual) surface (interface) area and A_g is the geometrical surface (interface) area. As shown in Fig. 3(A), the amount of surface oxide formed can be measured by integration of the Au oxide reduction peak in a cathodic scan (shadow area). The RF of the Au electrode is usually calculated in the basis of the electrochemically deposited oxygen monolayer on the surface of the electrode and the measurement of charge corresponding to the monolayer (Woods, 1976; Oesch and Janata, 1983). Since the charge/area ratio is different for the different planes of an Au-crystal, it is usually considered to be about 0.4 mC cm^{-2} for a regular polycrystalline Au electrode (Trasatti and Petrii, 1991). The accumulated charge density (18.42 mC cm^{-2}) in shadow area of Fig. 4(A) was divided by aforementioned charge density of the oxygen monolayer (0.4 mC cm^{-2}). Thus, the calculated RF of the macroporous Au electrode was approximately 46.07.

Meanwhile, the determination of the RF of the Pt electrode is based on the formation of a hydrogen monolayer electrochemically adsorbed at the surface of the electrode (Woods, 1976). As shown in Fig. 3B, Pt nanoparticles deposited on the surface of the macroporous Au electrode showed redox peaks, which is similar to what happens with a conventional Pt electrode. In Fig. 3(B), the first cathodic peak indicates the reduction of oxygen, which is quickly followed by the dual peak related to the reduction of hydrogen (shadow area). Since the charge is necessary to form a monolayer of adsorbed hydrogen and the electrode area is covered by each hydrogen atom, the electrochemical RF is easily calculated. The RF of the macroporous Au-/nPts is determined as the value of the adsorption charge divided by 0.21 mC cm^{-2} (Biegler et al., 1971). The accumulated charge density (425.18 mC cm^{-2}) in shadow area of Fig. 4(B) was divided by aforementioned charge density of the adsorbed hydrogen monolayer (0.21 mC cm^{-2}). The calculated RF was 2024.7, which was the highest value in the previous reported ones. This was caused by the synergistic effect of the macroporous Au structure and Pt nanoparticles. The result was also supported by the aforementioned FESEM images. Also, these results imply that the second metal is a crucial factor affecting the electrochemical activity of bimetallic nanocatalysts.

3.3. *Electrochemical measurements and the determination of free-cholesterol*

The voltammetric behaviors of the macroporous Au (Fig. 4A) and Au-/nPts (Fig. 4B) electrodes were obtained at a scan rate of 20 mV/s and the potential ranged from −0.4 V to 1 V *vs.* Ag/AgCl in 0.1 M PBS solution containing different concentrations of cholesterol (0, 1, 2, and 3 mM). Upon the addition of 1 mM cholesterol, the change in the oxidation currents for the macroporous Au and Au-/nPts electrodes at 0.3 V and 0.2 V was observed. The voltammetric response increased with increasing concentration of cholesterol as shown in Fig. 4. In both cases, the response currents evidently increased with increasing increments of cholesterol concentration, because of the increase in electron transfer force. Applied potentials of 0.3 V and 0.2 V would be used as working potentials for amperometric measurements. Low applied potentials are effective in the avoidance of direct oxidation of the AA and AP on the surface of the electrode.

Fig. 5A illustrates the amperometric responses of the macroporous Au and Au-/nPts electrodes towards the oxidation of cholesterol in PBS at 7.0 pH. Measurements at 50 s regular intervals were performed at potentials of 0.3 V and 0.2 V after stabilizing the background current at a nearly constant value. A 0.5 mM choles-

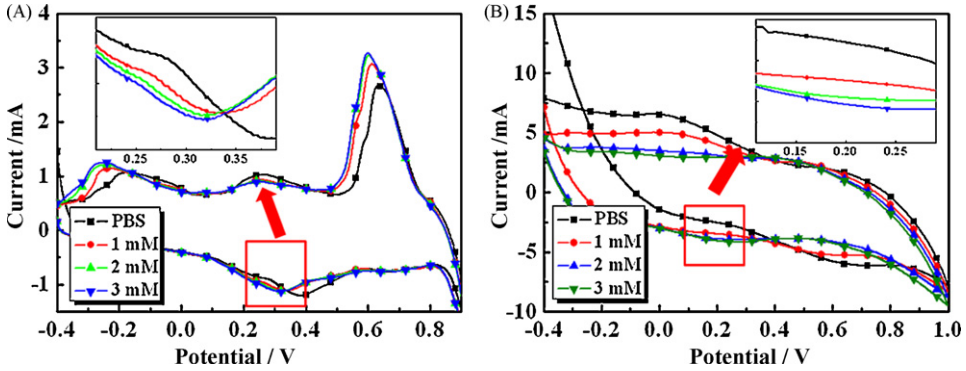

Fig. 4. Cyclic voltammograms of macroporous Au (A) and macroporous Au-/nPts (B) electrodes to various cholesterol concentrations (0, 1, 2, and 3 mM). Supporting electrolyte: 0.1 M PBS, pH 7.0; scan rate: 20 mV/s.

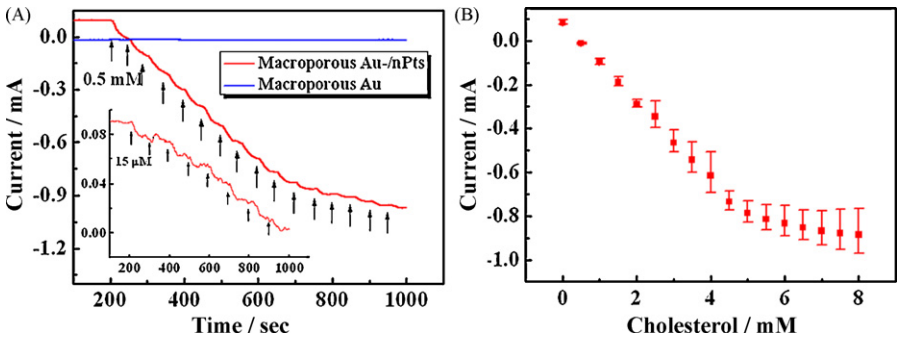

Fig. 5. Amperometric current responses of macroporous Au and Au-/nPts electrodes to successive addition of 0.5 mM cholesterol at 0.3 V and at 0.2 V of applied potential, respectively. Inset shows limit of detection of macroporous Au-/nPts (A) and calibration plot, concentration of cholesterol (up to 8 mM) *vs.* current for macroporous Au-/nPts (B).

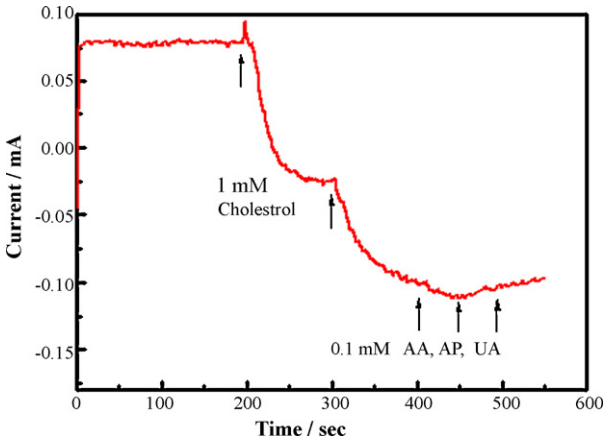

Fig. 6. Current–time curve of macroporous Au-/nPts electrode to the successive addition of 1 mM cholesterol, 0.1 mM AA, AP, and UA at 0.2 V of applied potential. Supporting electrolyte: 0.1 M PBS, pH 7.0.

terol solution was injected at regular 50 s intervals. As shown in Fig. 5A, the response current of the macroporous Au-/nPts gradually increased as the concentration of cholesterol increased. The response current increased linearly up to 5 mM cholesterol, and further increases in cholesterol concentration led to a slow rise of the current, whilst the response current of the macroporous Au electrode did not appear with incremental increase of the cholesterol concentration. This result indicates that the catalytic activity of the macroporous Au-/nPts towards cholesterol is caused by the Pt nanoparticles electroplated on the surface of the macroporous Au electrode. The lower left trace in Fig. 5(A) shows the amperometric response of the macroporous Au-/nPts to successive injections of cholesterol with a low cholesterol concentration. As indicated, the limit of detection was 0.015 mM. Fig. 5B shows a calibration curve obtained when the electrode is exposed to different concentrations of cholesterol. In order to test the repeatability of the free-cholesterol detection modified electrode, three electrodes were fabricated by the same method and measured in various cholesterol concentrations. In the linear range up to 5 mM, they exhibited a maximum relative standard deviation (RSD) value of 12.1%. Furthermore, the fabricated macroporous Au-/nPts are easily regenerated by electrochemical cleaning and chemically stable. Thus, it is suitable for non-disposable free-cholesterol sensor applications. The free-cholesterol sensitivity of the macroporous Au-/nPts was 226.2 $\mu A\,mM^{-1}\,cm^{-2}$ in the range up to 5 mM, which was much higher than the value reported in our previous work (Lee et al., 2009).

Fig. 6 shows the amperometric responses of the macroporous Au-/nPts to consecutive additions of a 1 mM cholesterol solution and a 0.1 mM solution of interfering species (e.g. AA, AP, UA) in a stirring PBS. One of the most important analytical factors for amperometric bio-molecule detection is the ability of the electrode to discriminate the interfering species having electroactivities similar to the target analyte. The oxidizable compounds such as AA, AP, and UA normally co-exist in real samples. The normal physiological level of cholesterol concentration is under 5.17 mM, which is much higher than the concentrations of interfering species like AA (0.1 mM), AP (0.1 mM), and UA (0.1 mM). As shown in Fig. 6, the response current of the macroporous Au-/nPts was stable and linear without being affected by the interfering species. Also, upon injection of cholesterol at regular intervals, a rapid increase in currents was observed.

4. Conclusions

In this paper, a new highly roughened and coral-like shaped macroporous Au electrode, obtained through the use of Pt nanoparticles has been reported. It has been characterized for its suitability for highly sensitive nonenzymatic free-cholesterol biosensor applications. A macroporous Au-/nPts was fabricated by the use of a templating method and electroplating technique. It was then characterized by the use of FESEM and cyclic voltammetric methods. The electrode showed a highly improved surface roughness factor, higher than all value previously reported. The highly roughened electrode surface of the macroporous Au-/nPts exhibited an extremely high sensitivity for cholesterol detection due to the enlarged activation surface area, without any redox mediator or enzyme and without being affected by interfering species as AA, AP, and UA. The electrochemically deposited Pt nanoparticles on the surface of the macroporous Au electrode led to significant improvement in the real surface activation area and it exhibited an extremely high sensitivity for cholesterol detection. In addition, it showed other attractive features such as a fast response. Thus, we believe than the new electrode will have strong applications in the development of nonenzymatic free-cholesterol biosensors.

Acknowledgements

This research was supported by the Seoul Research and Business Development Program (Grant No. 10583). The authors are grateful to MiNDaP (Micro/Nano Device & Packaging Lab.) group members of Department of Electronic Engineering and Prof. Y.H. Kim of Department of Chemical Engineering in Kwangwoon University for their technical supports.

References

Attard, G.S., Bartlett, P.N., Coleman, N.R.B., Elliott, J.M., Owen, J.R., Wang, J.H., 1997. Science 278, 838–840.

Biegler, T., Rand, D.A., Woods, R., 1971. J. Electroanal. Chem. 29, 269–277.
Bonnemann, H., Waldofner, N., 2002. Chem. Mater. 14, 1115–1120.
Boonyongmaneerat, Y., Saengkiettiyut, K., Saenapitak, S., Sangsuk, S., 2009. Surf. Coat. Technol. 203, 3590–3594.
Brahim, S., Narinesingh, D., Elie, A.G., 2001. Anal. Chim. Acta 448, 27–36.
Cao, J., Du, C., Wang, S.C., Mercier, P., Zhang, X., Yang, H., Akins, D.L., 2007. Electrochem. Commun. 9, 735–740.
Gloaguen, F., Leger, J.-M., Lamy, C., 1997. J. Appl. Electrochem. 27, 1052–1060.
Katsuaki, S., Ryuhei, I., Hideaki, K., 1990. J. Electroanal. Chem. 284, 523–529.
Khan, R., Kaushik, A., Mishra, A.P., 2009. Mater. Sci. Eng. 29, 1399–1403.
Kim, H., Kim, Y., Joo, J.B., Ko, J.W., Yi, J., 2009. Micropor. Mesopor. Mater. 122, 283–287.
Konishi, J., Fujita, K., Nakanishi, K., Hirao, K., 2006. Chem. Mater. 18, 6069–6074.
Kumar, A., Rajesh, Chaubey, A., Grover, S.K., Malhotra, B.D., 2001. J. Appl. Polym. Sci. 82, 3486–3491.
Lee, Y.-J., Park, D.-J., Park, J.-Y., Kim, Y., 2008. Sensors 8, 6154–6164.
Lee, Y.-J., Kim, J.-D., Park, J.-Y., 2009. J. Kor. Phys. Soc. 54, 1769–1773.
Loffler, M.-S., Grob, B., Natter, H., Hempelmann, R., Krajewski, Th., Divisek, J., 2001. Phys. Chem. Chem. Phys. 3, 333–336.
MacLachlan, J., Wotherspoon, A.T.L., Ansell, R.O., Brooks, C.J.W., 2000. J. Steroid Biochem. Mol. Biol. 72, 169–195.
Malhotra, B.D., Chaubey, A., 2003. Sens. Actuators B 91, 117–127.
Martin, S.P., Lamb, D.J., Lynch, J.M., Reddy, S.M., 2003. Anal. Chim. Acta 487, 91–100.
McNaught, A.D., Wilkinson, A., 1997. IUPAC Compendium of Chemical Terminology (the "Gold Book"), 2nd ed. Blackwell Scientific Publications, Oxford, 58 (1986) 437 (interphases in systems of conducting phases (Recommendations 1985)) on p. 439.
Oesch, U., Janata, J., 1983. J. Electrochim. Acta 28, 1237–1246.
Park, S.J., Boo, H.K., Chung, T.D., 2006. Anal. Chim. Acta 556, 46–57.
Shumyantseva, V., Deluca, G., Bulko, T., Carrara, S., Nicolini, C., Usanov, S.A., Archakov, A., 2004. Biosens. Bioelectron. 19, 971–976.
Solanki, P.R., Kaushik, A., Ansari, A.A., Tiwari, A., Malhotra, B.D., 2009. Sens. Actuators B 137, 727–735.
Srivastava, R.C., Sahney, R., Upadhyay, S., Gupta, R.L., 2000. J. Membr. Sci. 164, 45–49.
Szamocki, R., Velichko, A., Holzapfel, C., Mucklich, F., Ravaine, S., Garrigue, P., Sojic, N., Hempelmann, R., Kuhn, A., 2007. Anal. Chem. 79, 533–539.
Trasatti, S., Petrii, O.A., 1991. Pure Appl. Chem. 63, 711–734.
Woods, R., 1976. In: Bard, A.J. (Ed.), Electroanalytical Chemistry, vol. 9. Marcel Dekker, New York, p. 1.
Yu, J.-S., Kang, S., Yoon, S.B., Chai, G., 2002. J. Am. Chem. Soc. 124, 9382–9383.